JACS
JOURNAL OF THE AMERICAN CHEMICAL SOCIETY

Communication

pubs.acs.org/JACS

Re-examining the Size/Charge Paradigm: Differing in Vivo Characteristics of Size- and Charge-Matched Mesoporous Silica Nanoparticles

Jason L. Townson,[†,‡] Yu-Shen Lin,[†,‡] Jacob O. Agola,[†] Eric C. Carnes,[∥] Hon S. Leong,[#] John D. Lewis,[¶] Christy L. Haynes,[◆] and C. Jeffrey Brinker*[,†,§,⊥]

[†]Center for Micro-Engineered Materials, [§]Department of Chemical Engineering, the University of New Mexico, Albuquerque, New Mexico 87131, United States

[∥]Nanobiology Department, [⊥]Self-Assembled Materials Department, Sandia National Laboratories, Albuquerque, New Mexico 87185, United States

[#]London Regional Cancer Program, London, Canada

[¶]Department of Oncology, University of Alberta, Edmonton, Canada

[◆]Department of Chemistry, University of Minnesota, Minneapolis, Minnesota, 55455, United States

Supporting Information

ABSTRACT: The combination of nanoparticle (NP) size, charge, and surface chemistry (e.g., extent of modification with polyethylene glycol (PEG)) is accepted as a key determinant of NP/cellular interactions. However, the influence of spatial arrangement and accessibility of the charged molecules on the NP surface *vis-à-vis* the average surface charge (zeta (ζ) potential) is incompletely understood. Here we demonstrate that two types of mesoporous silica nanoparticles (MSNP) that are matched in terms of primary and hydrodynamic particle size, shape, pore structure, colloidal stability, and ζ potential, but differ in surface chemistry, *viz*. the spatial arrangement and relative exposure of surface amines, have profoundly different interactions with cells and tissues when evaluated *in vitro* and *in vivo*. While both particles are ∼50 nm in diameter, PEGylated, and positively charged (ζ = +40 mV), PEG-PEI (MSNPs modified with exposed polyamines), but not PEG-NMe_3^+ (MSNP modified with distributed, obstructed amines) rapidly bind serum proteins, diverse cells types *in vitro*, and endothelial and white blood cells *in vivo* (ex ovo chick embryo model). This finding helps elucidate the relative role of surface exposure of charged molecules vs ζ potential in otherwise physicochemically matched MSNP and highlights protein corona neutrality as an important design consideration when synthesizing cationic NPs for biological applications.

Nanoparticle (NP)/cell interactions, particularly in complex *in vivo* microenvironments, are regulated by an intricate spatiotemporal interplay of numerous biological and NP characteristics. Multiple NP physicochemical properties including, at the most basic level, material composition, size, shape, surface charge, and surface chemistry, have all been reported to play significant roles.[1−3] However, the relative importance of these diverse NP physicochemical properties in regulating interactions with various biological systems remains incompletely understood.[1] As such, achieving or avoiding cell-type-specific interactions *in vivo* requires an improved understanding of the relative roles of these diverse NP properties, as well an ability to exert a high level of control over these properties during NP synthesis. While the existing paradigm dictates that decreased size, neutral or negative zeta (ζ) potential, and extent of PEGylation are correlated with increased circulation time (i.e., reduced interaction with host cells),[4] the manner in which these combined physicochemical properties conspire to direct *in vivo* cellular interactions has not been elucidated through careful systematic studies, and the nature of these interactions is likely to vary significantly by particle formulation and cell type. As amination of particles is commonly used in various particle modification schemes to enable labeling or targeting, enhance binding and internalization,[5] etc., here we attempt to further elucidate how the exposure of surface amines affects interaction of PEGylated, colloidally stable MSNP with diverse cell types both *in vitro* and *in vivo*. In order to directly reveal the influence of amine accessibility on cellular interactions, we synthesized two types of MSNPs (studied extensively for NP-based drug delivery[6,7]) with nearly identical size, shape, pore structure, colloidal stability, PEGylation, and ζ potential, but differing in exposure and spatial distribution of amines on their surfaces.

It was found that despite the high degree of similarity between the particles (essentially indistinguishable by commonly employed transmission electron microscopy (TEM), dynamic light scattering (DLS), and ζ-potential measurements) exposure of even very low amounts of surface primary amines dominated the NP/cell interaction with serum proteins and cells *in vitro* and resulted in rapid clearance from circulation *in vivo* by interaction with endothelial and white blood cells (WBCs). Indeed, *in vivo*, amine accessibility (not ζ potential) was found to alter circulation and vascular binding properties to a significantly greater extent than NP size.

Received: August 13, 2013

   dx.doi.org/10.1021/ja4082414 | J. Am. Chem. Soc. XXXX, XXX, XXX−XXX

Table 1. Physicochemical Properties of PEG-PEI, PEG-NMe_3^+, and PEG-PEI-ace MSNPs

sample	D_h in DI water (nm)	D_h in PBS (nm)	D_h in DMEM (nm)	D_h in DMEM+ 10%FBS (nm)	ζ in DI water (mV)	ζ in 10 mM $NaCl_{(aq)}$ (mV)	ζ after DMEM+ 10% FBS incubation (mV)
PEG-PEI	59.0 ± 1.5	59.5 ± 2.3	59.5 ± 2.2	82.3 ± 3.8	+40.1 ± 3.0	+20.3 ± 2.8	−8.0 ± 3.1
PEG-NMe_3^+	60.1 ± 1.3	59.4 ± 1.5	59.9 ± 2.0	54.4 ± 1.9	+40.2 ± 2.1	+20.4 ± 3.5	+20.6 ± 3.5
PEG-PEI-ace	59.2 ± 2.4	58.4 ± 1.9	58.6 ± 1.8	54.9 ± 1.8	+17.8 ± 3.6	+5.5 ± 3.3	+7.8 ± 4.3

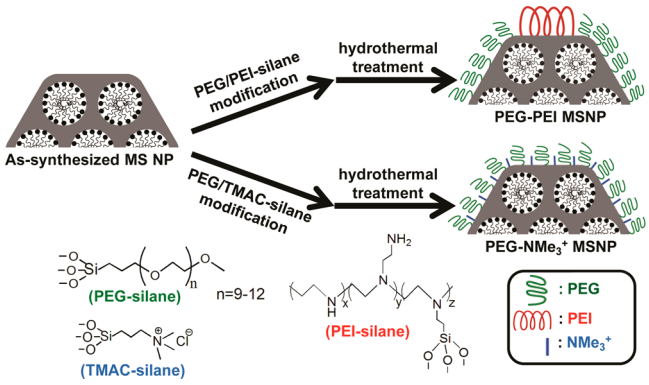

Figure 1. Schematic illustration of the design and synthesis of two positively charged PEGylated MSNPs, designated as PEG-PEI and PEG-NMe_3^+.

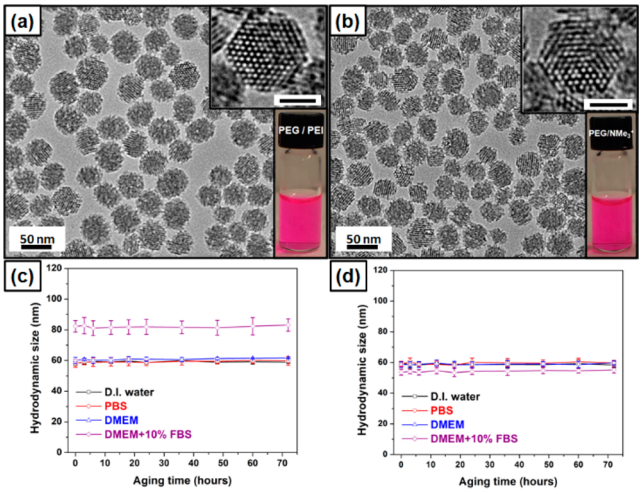

Figure 2. (a,b) TEM and optical images of rhodamine B-labeled PEG-PEI (a) and PEG-NMe_3^+(b) MSNPs following removal of surfactant, scale bar = 25 nm. (c,d) Hydrodynamic diameters of PEG-PEI (c) and PEG-NMe_3^+ (d) MSNP vs aging time in various solutions.

To address the relative effect of cationic molecule (amine) exposure on NP interaction with cells, fluorescently labeled MSNPs matched for size, shape, pore structure, PEGylation, and ζ potential (Figure 2, Table 1) were synthesized by modification of a hydrothermal-assisted method described previously[8] (see Supporting Information [SI]) using trimethoxy-silylpropyl-modified polyethyleneimine (MW = 1500−1800, PEI-silane, a branched cationic polymer composed of primary, secondary, and tertiary amines as identified in a previous study[9]), or *N*-trimethoxysilylpropyl-*N*,*N*,*N*-trimethyl ammonium chloride (TMAC-silane, MW 258) as the amination reagent (Figure 1) and 2-[methoxy(polyethyleneoxy)-propyl]trimethoxysilane (MW 550−750, 9−12 EO, PEG-silane) for MSNP PEGylation. Compared to alternative colloidal MSNP procedures,[10] this hydrothermal process drives more extensive condensation of silanes, minimizing surface exposure of silanol groups that, on their own, drive strong NP/cellular interactions.[11] By balancing the relative proportions of the branched, higher-molecular weight PEI-silane and lower-molecular weight TMAC-silane used in the respective synthesis procedures, we were able to prepare size- and charge-matched particles wherein, for PEG-PEI, we expect the higher molecular weight of the branched PEI to expose primary amines beyond the PEG layer, while for PEG-NMe_3^+ MSNPs, the quaternary amine of the hydrolyzed TMAC-silane is expected to be more uniformly distributed and partially obstructed within the PEG layer (Figure 1).

TEM imaging and DLS measurements revealed that the basic particle size, shape, pore structure, hydrodynamic size in various solutions, and colloidal stability were nearly identical between those of PEG-PEI and PEG-NMe_3^+ MSNPs (Figure 2, Table 1, and Figure S1 in the SI). Additionally, ζ potential measurements indicated the particles to be cationic and charge matched (ζ = +40 mV and +20 mV measured in DI water and 10 mM $NaCl_{(aq)}$, respectively (Table 1 and Figure S2 [SI]). Pore size and total surface area as measured by nitrogen sorption for both particles were ∼2 nm and ∼500 m^2/g, respectively (Figure S3 and Table S1 in SI). Measurement of hydrodynamic diameter by DLS in various solutions over time revealed that, while the particles were colloidally stable and nearly identical in diameter when measured in water, PBS, and cell culture medium, an instantaneous ∼20 nm increase in hydrodynamic diameter was observed for only PEG-PEI particles when incubated in medium containing serum (Figure 2c and Figure S4 in SI, and Table 1).

This increase in diameter and change in ζ potential (+40 to −8 mV, Table 1) is attributed to the formation of a protein corona and indicates that, despite their nearly indistinguishable physicochemical parameters routinely measured to assess and predict biomolecular interactions, size-, shape-, and charge-matched particles can behave differently in even the most simplified mimic of biological conditions. Given that for comparably PEGylated NPs the combined size and charge are thought to be predominant factors dictating NP/cellular interactions such as nonspecific binding and internalization,[4] and that cationic NPs in particular show high degrees of nonspecific binding and in some cases toxicity,[3] we exposed multiple cell types to PEG-PEI and PEG-NMe_3^+ MSNP. As evident in fluorescence microscopy images in Figure 3a−c, PEG-PEI particles bind strongly to A549 (human lung carcinoma), A431 (human epithelial cancer), Hep3B (human hepatocellular carcinoma), and human hepatocytes following 30-min exposure (10 μg/mL) under normal cell culture conditions. In contrast, and unexpectedly for a cationic NP, PEG-NMe_3^+ particles exhibit minimal binding to all cell types under the same conditions (Figures 3b,d and S5 in SI). NP binding observed via fluorescence microscopy was confirmed and quantified by flow cytometry (Figures 3d and S5). Although in all cases PEG-PEI MSNPs demonstrated significantly increased binding relative to PEG-NMe_3^+ particles, it should be noted that, at the same concentration of NPs, hepatocytes exhibited decreased binding to PEG-PEI particles relative to other cell lines (Figure S5).

dx.doi.org/10.1021/ja4082414 | J. Am. Chem. Soc. XXXX, XXX, XXX−XXX

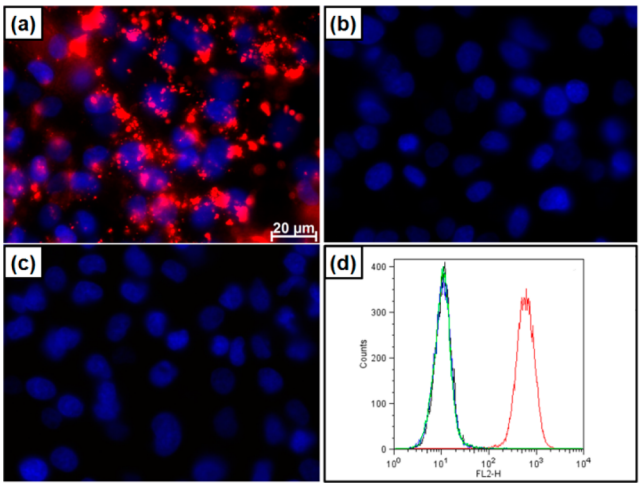

Figure 3. Differential binding of red fluorescently labeled PEG-PEI, PEG-NMe_3^+, and PEG-PEI-ace particles to A549 cells *in vitro*. PEG-PEI (a) but not PEG-NMe_3^+ (b) or PEG-PEI-ace (c) particles are observed to bind to A549 cells (blue - dapi stained nuclei) via fluorescent microscopy. Particle binding is confirmed by flow cytometry (d). PEG-PEI (red), PEG-NMe_3^+ (blue), PEG-PEI-ace (green), and cells only (black).

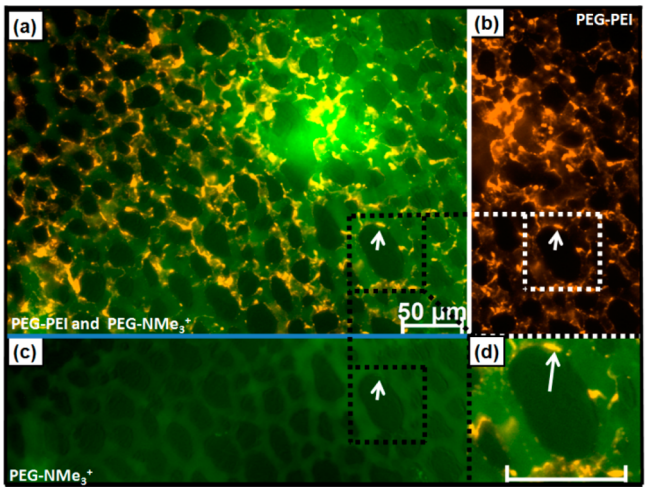

Figure 4. Differential *in vivo* binding and flow of size- and charge-matched PEG-PEI (orange) and PEG-NMe_3^+ (green) MSNP in chick CAM 10-min post injection. (a) Merged image, (b) PEG-PEI showing arrest on endothelial cells, and (c) PEG-NMe_3^+ image showing circulating MSNPs. (d) Magnification of PEG-PEI MSNP binding (arrow) on endothelial cells (scale bar 50 μm).

While our primary goal was to elucidate the effect of amine exposure on NP/cellular interactions, this observation highlights the capability of the cell itself to regulate binding that would typically be classified as "non-specific" (i.e., no specific ligand targeting and based on generally ubiquitous charge or chemical interactions) and could be a result of variance in cellular membrane potential as recently described.[12] As the exposed primary amines on the PEG-PEI particles were hypothesized to be responsible for the greatly enhanced binding of otherwise size-, charge-, and PEG-matched particles, primary amines on the PEG-PEI particle were neutralized by titration with acetic anhydride (see SI: the acetylated PEG-PEI MSNPs are designated as PEG-PEI-ace). As expected, acetylation of the primary amines reduced the ζ potential, measured to be +20 mV in DI water and +5 mV in 10 mM $NaCl_{(aq)}$ (Table 1). However the particles were shown to be colloidally stable and exhibited no increase in size when introduced into various solutions, including medium with serum (Table 1 and Figure S4). Furthermore, we observed that elimination of primary amines completely inhibited nonspecific particle binding to various cell types (Figures 3c,d and S5). In all cases, no toxicity was observed[5] with any cell/particle combination after 24 h incubation at various concentrations (12.5−200 μg/mL) as assessed via water-soluble tetrazolium salt (WST-8), lactate dehydrogenase (LDH), (Figure S6) and hemolysis assays (Figure S7) conducted with human red blood cells (RBCs). These results indicate both PEG-PEI and PEG-NMe_3^+ are highly biocompatible.

While it was anticipated that cationic NPs would bind most cell types,[2,3,14,15] the relative importance of the exposed amines in otherwise physicochemically matched particles is not generally recognized. Indeed, the lack of binding of cationic PEG-NMe_3^+ (+40 mV) was unanticipated despite the presence of PEG. However, the NP binding studies reported in Figure 3 were conducted *in vitro* without the multitude of competing biological factors found in most *in vivo* systems. To investigate whether this dramatic differential cellular binding occurs in a complex *in vivo* system (with blood proteins and cells, endothelial cells, sinusoidal tissue, fenestrated capillaries, a mononuclear phagocyte system, velocity changes, shear forces, etc.), we injected 50 μg of 50 nm PEG-PEI, PEG-NMe_3^+, or PEG-PEI-ace NPs into veins of *ex ovo* chick embryos as described previously.[13] This model allows for high-resolution, real-time, *in vivo* imaging of particle interactions with various cell types and tissues observed within the chorioallantoic membrane (CAM), including WBCs, RBCs, and endothelial cells. A representative video of CAM blood flow and vascular architecture is provided as Video S1 ja4082414_si_002, and representative videos of PEG-PEI and PEG-NMe_3^+ circulation and binding are respectively provided in Videos S2 and S3, ja4082414_si_003 and ja4082414_si_004. Co-injection of PEG-PEI and PEG-NMe_3^+ particles revealed a dramatic alteration in the fate of these size- and charge-matched particles (Figure 4). Immediately following particle injection, PEG-PEI MSNPs (orange) were observed to bind to endothelial cells and stationary and circulating WBCs, as apparent by the fluorescence intensity on the perimeter of the capillary vessels (endothelial cells) as well as more globular/punctate features (WBCs). In contrast, PEG-NMe_3^+ MSNPs (Figure 4a - green) remained in circulation for ≫6 h post injection (Figure S8c). Additionally, the location of vascular deposition shifted, with PEG-PEI particles primarily observed in capillaries and bound to WBCs, while PEG-NMe_3^+ particles accumulated very slowly in venules and were taken up more slowly by WBCs (Figure S8c). PEG-PEI-ace particles exhibited circulation and accumulation patterns similar to those of PEG-NMe_3^+ particles, with minimal immediate or delayed deposition within the capillary bed (Figure S8d). The importance of amine exposure was further tested by injection of $PEG_{650/5k}$-PEI particles synthesized with a 50% substitution of the MW 550−750 PEG with larger (MW = 5000) PEG-silane (see SI). Shielding of the amine resulted in a reduction of immediate binding to the CAM endothelium and WBCs (Figure S9 [SI]) similar to that observed for acetylation.

This preferential binding of PEG-PEI particles to the capillary endothelium and uptake by WBCs necessarily reduces the concentration of circulating NPs and diminishes binding to cancer cells *in vivo* (Figure S10) relative to that observed *in vitro* (Figure 3). Figure S10 shows capillary vascular and WBC binding of PEG-PEI with no apparent binding (relative to background)

dx.doi.org/10.1021/ja4082414 | J. Am. Chem. Soc. XXXX, XXX, XXX−XXX

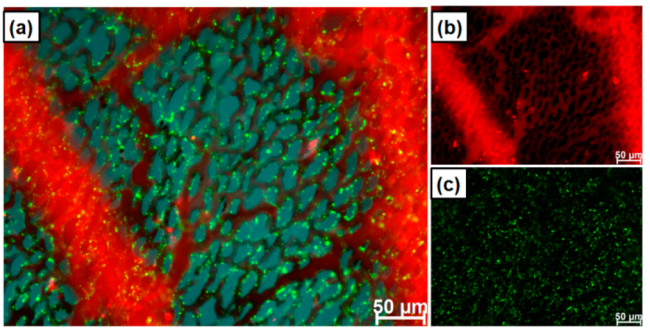

Figure 5. Size vs exposed amine-mediated binding. PEG-PEI MSNPs, 50 nm (green, +40 mV), were observed to bind to endothelial cells immediately after injection. PEG-NMe_3^+ MSNPs, 150 nm (red, +40 mV), circulated for hours post injection. (a) Merged image, (b) 150 nm PEG-NMe_3^+, (c) 50 nm PEG-PEI. (The field of view of b and c is the same as that of a.)

to fluorescently labeled A431 cancer cells injected 30 min prior to particle injection. This highlights that *in vitro* binding—with no competing factors—is not a reliable predictor of *in vivo* behavior and that PEG-PEI particles bind preferentially to the capillary endothelium and, presumably due to immediate protein corona formation, are rapidly scavenged by WBCs. Similar to the reduction of PEG-PEI particle binding observed on hepatocytes relative to other cell types *in vitro*, neither PEG-PEI nor PEG-NMe_3^+ showed nonspecific binding to RBCs as confirmed *ex vivo* by imaging of isolated RBCs (Figure S11). Our findings emphasize the complexity in regulation of even nonspecific binding *in vivo*.

To establish the relative importance of size vs exposed charge on biodistribution and immediate endothelial binding, 150-nm RITC-labeled PEG-NMe_3^+ (TEM images, hydrodynamic size, and ζ potential shown in Figure S12 and Table S2 [SI] were synthesized and coinjected with charge-matched 50-nm PEG-PEI particles. Despite the tripling in diameter and ∼27-fold increase in mass, 150-nm PEG-NMe_3^+ exhibited relatively little immediate binding to the capillary endothelium or scavenging by WBC when compared to 50 nm PEG-PEI particles (Figure 5). These results demonstrate that accessible primary amines play a significant role in regulating NP/cell interactions, overwhelming the role of particle size.

Through synthesis of two types of MSNPs that are matched in terms of primary and hydrodynamic particle size, shape, pore structure, colloidal stability, and ζ potential, our *in vitro* and *in vivo* studies have elucidated the relative importance of charged molecule exposure and spatial arrangement vs ζ potential and/or particle size as determinants of nonspecific binding and biodistribution. Uniform spatial distribution of charge presented within a PEG background for PEG-NMe_3^+ confers both colloidal stability and protein corona neutrality, which in turn correlate with minimal nonspecific binding *in vivo* and prolonged circulation (and potentially opsonization neutrality), as evidenced by DLS. Such NP characteristics are expected to be ideal for maximizing the enhanced permeability and retention (EPR) effect or for binding and delivery to targeted circulating cells. In contrast, charge-matched PEG-PEI particles displaying surface-exposed, branched amines, although colloidally stable, immediately form a protein corona and exhibit rapid nonspecific binding to endothelial and WBCs and arrest within the CAM. These characteristics are of potential interest for in vivo WBC and vascular labeling. It is also apparent that the combination of size and charge alone are poor predictors of *in vivo* behavior, and we suggest charge exposure and its effect on protein corona formation and WBC scavenging should be considered additionally when designing NPs for *in vivo* applications.

■ ASSOCIATED CONTENT

Ⓢ Supporting Information

Experimental details and additional data and movies, ja4082414_si_002, ja4082414_si_003, and ja4082414_si_004. This material is available free of charge via the Internet at http://pubs.acs.org.

■ AUTHOR INFORMATION

Corresponding Author

cjbrink@sandia.gov

Author Contributions

‡J.L.T. and Y.-S.L. contributed equally.

Notes

The authors declare no competing financial interest.

■ ACKNOWLEDGMENTS

We thank Walker Wharton and Katharine Epler for helpful discussions and experimental assistance. This work was funded by NIH Grant UO1 CA151792-01. J.L.T. was supported by a Young Investigators Award from Gabrielle's Angel foundation. Y.S.L. was funded by a fellowship from The UNM CNTC. C.J.B acknowledges additional support from U.S. DOE, Office of Basic Energy Sciences, Division of Materials Sciences and Engineering, Sandia National Laboratories' LDRD program, AFOSR grant FA 9550-10-1-0054, NSF and EPA.

■ REFERENCES

(1) Nel, A. E.; Madler, L.; Velegol, D.; Xia, T.; Hoek, E. M. V.; Somasundaran, P.; Klaessig, F.; Castranova, V.; Thompson, M. *Nat. Mater.* **2009**, *8*, 543.
(2) Albanese, A.; Tang, P. S.; Chan, W. C. W. *Annu. Rev. Biomed. Eng.* **2012**, *14*, 1.
(3) Dobrovolskaia, M. A.; Aggarwal, P.; Hall, J. B.; McNeil, S. E. *Mol. Pharmaceutics* **2008**, *5*, 487.
(4) Wang, J.; Byrne, J. D.; Napier, M. E.; DeSimone, J. M. *Small* **2011**, *14*, 1919.
(5) Rosenholm, J. M.; Meinander, A.; Peuhu, M.; Niemi, R.; Eriksson, J. E.; Sahlgren, C.; Linden, M. *ACS Nano* **2009**, *3*, 197.
(6) Tarn, D.; Ashley, C. E.; Xue, M.; Carnes, E. C.; Zink, J. I.; Brinker, C. J. *Acc. Chem. Res.* **2013**, *46*, 792.
(7) Lin, Y.-S.; Hurley, K. R.; Haynes, C. L. *J. Phys. Chem. Lett.* **2012**, *3*, 364.
(8) Lin, Y.-S.; Abadeer, N.; Hurley, K. R.; Haynes, C. L. *J. Am. Chem. Soc.* **2011**, *133*, 20444.
(9) Dacarro, G.; Cucca, L.; Grisoli, P.; Pallavicini, P.; Patrini, M.; Taglietti, A. *Dalton Trans.* **2012**, *41*, 2456.
(10) Lai, C.-Y.; Trewyn, B. G.; Jeftinija, D. M.; Jeftinija, K.; Xu, S.; Jeftinija, S.; Lin, V. S.-Y. *J. Am. Chem. Soc.* **2003**, *125*, 4451.
(11) Zhang, H.; Dunphy, D. R.; Jiang, X.; Meng, H.; Sun, B.; Tarn, D.; Xue, M.; Wang, X.; Lin, S.; Ji, Z.; Li, R.; Garcia, F. L.; Yang, J.; Kirk, M. L.; Xia, T.; Zink, J. I.; Nel, A. E.; Brinker, C. J. *J. Am. Chem. Soc.* **2012**, *134*, 15790.
(12) Shin, E. H.; Li, Y.; Kumar, U.; Sureka, H. V.; Zhang, X.; Payne, C. K. *Nanoscale* **2013**, *5*, 5879.
(13) Leong, H. S.; Steinmetz, N. F.; Ablack, A.; Destito, G.; Zijlstra, A.; Stuhlmann, H.; Manchester, M.; Lewis, J. D. *Nat. Protoc.* **2010**, *5*, 1406.
(14) Slowing, I.; Trewyn, B. G.; Lin, V. S.-Y. *J. Am. Chem. Soc.* **2006**, *128*, 14792.
(15) Chung, T. H.; Wu, S. H.; Yao, M.; Lu, C. W.; Lin, Y. S.; Hung, Y.; Mou, C. Y.; Chen, Y. C.; Huang, D. M. *Biomaterials* **2007**, *28*, 2959.